Doppler-free Yb spectroscopy with the fluorescence spot technique

Altaf H. Nizamani, James J. McLoughlin, and Winfried K. Hensinger[*]

Department of Physics and Astronomy, University of Sussex, Falmer, Brighton, East-Sussex, BN1 9QH, United Kingdom
(Received 18 June 2010; published 8 October 2010)

We demonstrate a simple technique to measure the resonant frequency of the 398.9-nm $^1S_0 \leftrightarrow {}^1P_1$ transition for the different Yb isotopes. The technique, which works by observing and aligning fluorescence spots, has enabled us to measure transition frequencies and isotope shifts with an accuracy of 60 MHz. We provide wavelength measurements for the transition that differ from previously published work. Our technique also allows for the determination of Doppler-shifted transition frequencies for photoionization experiments when the atomic beam and the laser beam are not perpendicular and furthermore allows us to determine the average velocity of the atoms along the direction of the atomic beam.

I. INTRODUCTION

Ytterbium, both atomic and singly ionized, is an element widely used in experiments involving trapped atoms and ions, such as laser cooling and trapping of neutral atoms and ions [1–12], atomic clocks [13–16], frequency standards [17–20], quantum computing experiments [21,22], quantum optics [23], and atomic parity nonconservation experiments [24]. Knowledge of the $^1S_0 \leftrightarrow {}^1P_1$ transition line in atomic Yb and of the corresponding frequency shifts for the stable isotopes is very important in these experiments as it allows for laser cooling and isotope selective photoionisation [20,22,25–27]. Various methods have been used to investigate these transitions and the corresponding isotope shifts [28–32].

We present our measurements of the ytterbium $^1S_0 \leftrightarrow {}^1P_1$ transition frequencies which differ from previously published results [29]. Using a simple method based upon observing and aligning fluorescence spots of atomic Yb generated from an atomic oven in an evacuated glass bell jar, we measured resonant transition frequencies and isotope shifts to an accuracy of 60 MHz. Our results were compared to the results obtained using saturation absorption spectroscopy and were further verified by ionizing and trapping Yb ions.

The advantage of our technique is that it can be used to determine resonance frequencies when the atomic beam is not necessarily perpendicular to the propagation of the laser, which can be the case in many experiments. These Doppler shifts also depend on the mean velocity of the atomic beam, so the measurement is quite useful. Using our technique we were able to measure the Doppler shift of the transition frequency under a range of angles and then derive the average velocity of the atoms along the direction of the atomic beam.

II. EXPERIMENTAL SETUP

To drive the $^1S_0 \leftrightarrow {}^1P_1$ 399-nm dipole transition an inexpensive in-house-built ultraviolet external cavity diode laser (ECDL) was used. The ECDL was formed with a laser diode (frequency selected to 399 nm; Sanyo diode, DL-4146-301S) and a diffraction grating (Newport, 53-*-240R) positioned in the Littrow configuration. A piezo electric actuator was used to adjust the angle of the grating and thus tuning the emission wavelength. To stabilize the emission wavelength a High Finesse wavelength meter (WS-07, with a specified wavelength accuracy of 60 MHz) and NI-DAQ cards operating under labVIEW real time were used. The wavemeter is calibrated using a 780-nm laser which is locked to within 1 MHz of the ^{87}Rb D_2 line. It measures the wavelength of the ECDL and sends the information to a labVIEW program, via an NI-DAQ Card (NA-6143). The program determines a drift in wavelength and generates the corresponding error signal to keep the laser stable.

To perform saturation spectroscopy on the $^1S_0 \leftrightarrow {}^1P_1$ 399-nm isotope transitions the ECDL frequency was required to scan over a range of 3 GHz. However, adjustment of the grating angle alone in the ECDL resulted in a mode-hop-free tuning range of only 800 MHz. To overcome this the piezo voltage and laser diode current were adjusted simultaneously to produce a mode-hop-free tuning range of over 5.5 GHz. For our technique an atomic flux propagating in a known direction was required as this enabled localized fluorescence spots that could be be spatially resolved. To generate the Yb atomic beam a resistively heated stainless steel oven tube (2 cm long and 1.5 mm in diameter) was used. A small piece of natural Yb was placed inside the oven and the Yb atomic beam could be obtained by running an electric current of 5 to 6 A over the oven. The atomic oven was placed inside a vacuum chamber maintained at a pressure on the order of 10^{-8} torr.

III. FLUORESCENCE SPOT TECHNIQUE

We have devised a simple method that works by observing fluorescence spots produced by laser-atom interaction at resonant wavelengths. The experimental setup for our spot method can be seen in Fig. 1: here two pairs of nonoverlapping counterpropagating laser beams (each with an intensity of approximately 4.5 mW cm^{-2}) are passed through an atomic beam. For orientation the cylindrical axis of the oven tube is considered as the reference axis and the lasers are aligned perpendicular to this reference axis unless otherwise stated.

The atoms from the oven interact with the four laser beams producing four fluorescence spots. In the frame of reference of laser beam propagation each laser interacts with atoms of

—————
[*]W. K. Hensinger@sussex.ac.uk; URL: http://www.sussex.ac.uk/physics/iqt
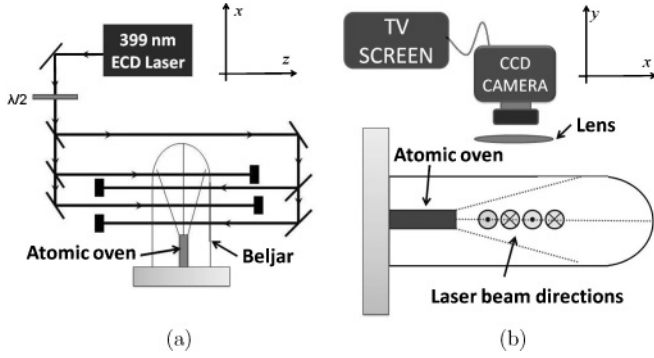
FIG. 1. Schematic diagram showing (a) the counterpropagating laser beams crossing the atomic beam and (b) the direction of the laser beams and the TV-camera setup.

the same velocity group. When viewed in the laboratory frame the four spots are seen to be misaligned when the frequency is detuned from resonance, but when on resonance the four spots are seen to align perpendicular to the propagation of the laser beams. In this situation each laser is interacting with atoms of zero velocity perpendicular to the atomic beam. Spot alignment can be seen in Fig. 2, where 2(b) corresponds to when the laser frequency is on resonance and 2(a) and 2(c) correspond to when the laser frequency is detuned -20 and $+20$ MHz from resonance, respectively. This phenomenon occurs irrespective of the angle between the cylindrical axis of the ovens and the laser beams, which is discussed later.

In order to obtain the $^1S_0 \leftrightarrow {}^1P_1$ transition frequencies, the frequency of the 399-nm laser diode was scanned slowly over 3 GHz. During the scan the florescence spots were imaged using an inexpensive CCD camera setup. After narrowing down the scanning range, the frequencies of the transitions of the different isotopes were individually measured by aligning the four spots in a straight line with the cylindrical axis of the atomic oven. This is shown in Fig. 2. We have measured the frequency of the $^{174}\text{Yb}\,{}^1S_0 \leftrightarrow {}^1P_1$ transition to be 751.526 65 THz $\pm$ 60 MHz, which disagrees with a previously published value of 751.525 987 761 THz $\pm$ 60 kHz [29] by approximately 660 MHz. Das *et al.* [29] relied in their measurement on the stated accuracy of 20 MHz of a home-built wavemeter and we speculate that the uncertainty of that wavemeter was larger than anticipated by the authors. Our measurement differs from the NIST Atomic Spectra Database [33] by 260 MHz, which lists the energy of the Yb $^1P_1$ level at 25 068.222 cm^{-1} (751.526 39 THz). If we examine this discrepancy more closely, we see that the database lists Meggers and Tech [28] as the most recent

source of their data. However, Meggers and Tech [28] list the level energy at 25 068.227 cm^{-1} (751.526 54 THz) which is only 110 MHz away from our measurement, pointing to a possible typographical error on the NIST Atomic Spectra Database. Considering that Meggers and Tech [28] used a natural mixture of Yb isotopes, their result is consistent with our measurement. We also note that the result by Meggers and Tech [28] shows an expected 550-MHz discrepancy with the measurement by Das *et al.* [29]. Using our measurements the isotope shifts relative to the $^{174}\text{Yb}\,{}^1S_0 \leftrightarrow {}^1P_1$ transition were then calculated. Our results are shown in Table I along with recently published results. The frequency shifts between the $^{172}\text{Yb}\,{}^1S_0 \leftrightarrow {}^1P_1$, $^{173}\text{Yb}\,{}^1S_0(F = 1/2) \leftrightarrow {}^1P_1(F = 3/2)$, and $^{173}\text{Yb}\,{}^1S_0(F = 1/2) \leftrightarrow {}^1P_1(F = 7/2)$ transitions are 18 and 55 MHz respectively, while the separation between the $^{170}\text{Yb}\,{}^1S_0 \leftrightarrow {}^1P_1$ and the $^{171}\text{Yb}\,{}^1S_0(F = 1/2) \leftrightarrow {}^1P_1(F = 1/2)$ transitions is 38 MHz [29]. These close transitions result in overlapping of the fluorescence spots and cannot be resolved by the spot method. The isotope-shift data presented in Table I for the Yb $^1S_0 \leftrightarrow {}^1P_1$ transitions are in very good agreement with previously published work [27,29–31].

A. Error analysis

To determine the resonant frequencies and isotope shifts we used the WS7 wavemeter from High Finesse (specified to 60 MHz accuracy). The wavemeter is calibrated using a 780-nm laser which is locked to within 1 MHz of the ^{87}Rb D_2 line. A He-Ne laser (SIOS SL02/1 calibrated to 1 MHz) was then used to provide confirmation of the calibration. A further two-point check was performed to ensure calibration in the ultraviolet frequency range. Using our frequency doubling system, which converts 739-nm light into 369-nm light, we measured the two wavelengths simultaneously and confirmed the wavemeter to operate within specifications. The wavemeter was calibrated before and after measurements and no changes in calibration measurements were observed. The wavemeter is specified to have an accuracy of 60 MHz for absolute frequency measurements, but is more accurate for relative frequency measurements of closely spaced transitions. For the 399-nm transitions, the relative accuracy is translated to be 20 MHz. Therefore the error on transition frequencies is 60 MHz and the error on isotope shifts is 30 MHz. However due to the actual line width of 20 MHz of these transitions and the resulting overlap of some transition lines, the isotope shift could not be resolved better than 60 MHz.

Other sources of error include nonparallel alignment of the lasers where beam misalignment of 1° related to 15 MHz error on wavelengths. As the technique can resolve a 20-MHz detuning from resonance it was possible to align
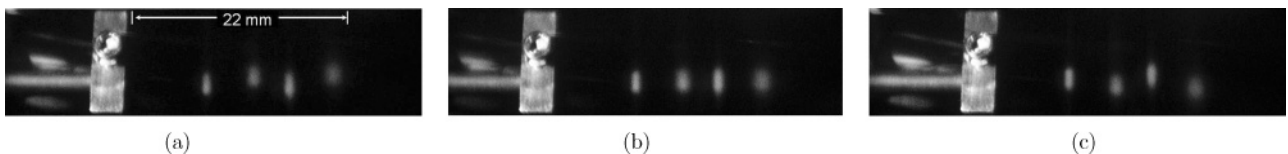

FIG. 2. Illustration of the resolution of the spectroscopy method. Pictures show the atomic ovens and fluorescence spots where the laser beams intersect the atomic beam; they were taken with the laser frequency (b) on resonance and detuned (a) -20 MHz and (c) $+20$ MHz from resonance.

TABLE I. The frequency shifts for the various isotopes of Yb from the ^{174}Yb $^1S_0 \leftrightarrow {}^1P_1$ transition line. The values were obtained from the fluorescence spot technique and compared with the previous published work.

Shift from ^{174}Yb (MHz)						
Isotope	Transition	This work	Ref. [29]	Ref. [30]	Ref. [27]	Ref. [31]
168	$^1S_0 \leftrightarrow {}^1P_1$	1883 ± 30	1887.400 ± 0.05			1870.2 ± 5.2
170[a]	$^1S_0 \leftrightarrow {}^1P_1$	1149 ± 60	1192.393 ± 0.066	1175.7 ± 8.1		1172.5 ± 5.7
171[a]	$^1S_0(F = 1/2) \leftrightarrow {}^1P_1(F = 1/2)$	1149 ± 60	1153.696 ± 0.061	1151.4 ± 5.6	1104 ± 69	1136.2 ± 5.8
171	$^1S_0(F = 1/2) \leftrightarrow {}^1P_1(F = 3/2)$	829 ± 30	832.436 ± 0.05	832.5 ± 5.6	822 ± 51	834.4 ± 4.0
172[a]	$^1S_0 \leftrightarrow {}^1P_1$	546 ± 60	533.309 ± 0.053	527.8 ± 2.8	534 ± 33	
173[a]	$^1S_0(F = 1/2) \leftrightarrow {}^1P_1(F = 3/2)$	546 ± 60	515.972 ± 0.2			
173[a]	$^1S_0(F = 1/2) \leftrightarrow {}^1P_1(F = 7/2)$	546 ± 60	587.986 ± 0.056	578.1 ± 5.8		
173	$^1S_0(F = 1/2) \leftrightarrow {}^1P_1(F = 5/2)$	-264 ± 30	-253.418 ± 0.05		-262 ± 16	
176	$^1S_0 \leftrightarrow {}^1P_1$	-509 ± 30	-509.310 ± 0.05	-507.2 ± 2.5		-554 ± 35

[a]Cannot be resolved with the spot method.

the lasers to better than $1°$ as misalignment would result in a visible deviation of the spots. Power broadening of the transition line was insignificant as each beam was less than 4.5 ± 0.9 mW cm^{-2} whereas the saturation intensity of the transition is 60 mW cm^{-2}, which translates to a 3-MHz linewidth broadening. The potential resolution of the technique can be seen from Fig. 2 where the frequency of the laser has been detuned from (b) resonance by (a) -20 MHz and (c) $+20$ MHz. The separation from the front of the oven to the furthest spot is approximately 22 mm, and by observing spot misalignment at a given detuning we extrapolate that the resolution of the technique can be 10 MHz in this particular setup.

IV. SATURATION ABSORPTION SPECTROSCOPY

To provide a comparison for the transition frequencies and isotope shifts obtained by our spot method, a typical saturation absorption spectroscopy experiment was set up. The saturation spectroscopy setup consisted of a pump and a probe beam (127 and 2 mW cm^{-2}, respectively) counterpropagating and overlapping through a ytterbium atomic beam. By scanning the wavelength of the external cavity diode laser the saturation plot shown in Fig. 3 was produced. The light-gray dashed line represents the Doppler background, which was
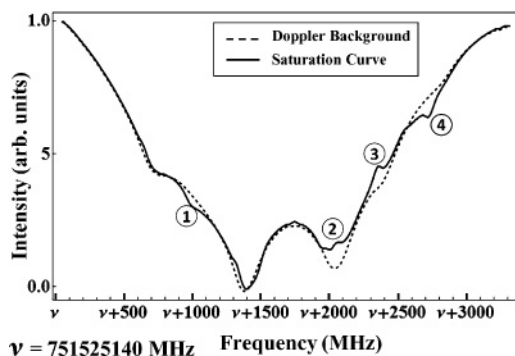
obtained by scanning the wavelength but blocking the pump beam. With the pump beam included the dark trace was produced. Saturation peaks for different isotopes can be seen at labels 1, 2, 3, and 4 on the graph and the corresponding frequencies are listed in Table II and compared with the results obtained with the spot method. It can be seen that the results obtained from the saturation spectroscopy are in good agreement with the results from our fluorescence spot method. However, the signal-to-noise ratio using the saturation spectroscopy setup is poor compared to that of the spot method. Furthermore, saturation spectroscopy can only be used to determine the resonant transition frequencies but not Doppler-shifted transition frequencies in nonperpendicular laser-atomic beam configurations which can be useful in ion-trap experiments.
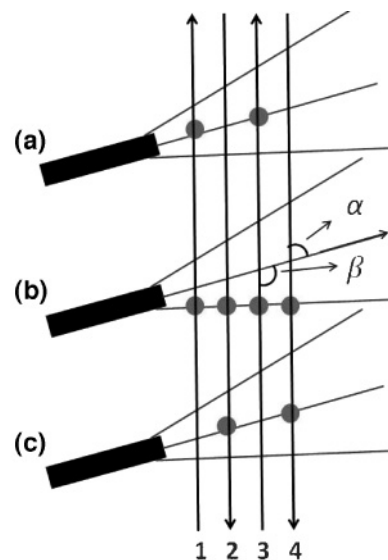
FIG. 3. $^1S_0 \leftrightarrow {}^1P_1$ transition peaks for different isotopes of Yb obtained with saturation absorption spectroscopy. The transitions corresponding to labels 1 to 4 are shown in Table II. The dashed line represents the Doppler background.

FIG. 4. Illustration of the counterpropagating laser beam pairs making an angle with the atomic beam. Laser beams 2 and 4 make an acute angle α and beams 1 and 3 make an obtuse angle β with the reference axis. To align the pair of spots with the reference axis, laser frequency is blue detuned in (a) and red detuned in (c). In (b) both spot pairs are aligned (but not with the reference axis) when the frequency is at resonance.

TABLE II. The absolute frequencies for the $^1S_0 \leftrightarrow {}^1P_1$ transition line of Yb isotopes obtained by saturation spectroscopy and the spot technique.

Peak	Yb Isotope	Transition	Frequency (THz) (Saturation)	Frequency (THz) (Spot method)
1	176	$^1S_0 \leftrightarrow {}^1P_1$	751.526 15(60)	751.526 15(60)
2	172[a]	$^1S_0 \leftrightarrow {}^1P_1$	751.527 14(120)	751.527 20(120)
	173[a]	$^1S_0(F = 1/2) \leftrightarrow {}^1P_1(F = 3/2)$	751.527 14(120)	751.527 20(120)
	173[a]	$^1S_0(F = 1/2) \leftrightarrow {}^1P_1(F = 7/2)$	751.527 14(120)	751.527 20(120)
3	171	$^1S_0(F = 1/2) \leftrightarrow {}^1P_1(F = 3/2)$	751.527 60(60)	751.527 49(60)
4	170[a]	$^1S_0 \leftrightarrow {}^1P_1$	751.527 79(120)	751.527 80(120)
	171[a]	$^1S_0(F = 1/2) \leftrightarrow {}^1P_1(F = 1/2)$		

[a]Not resolved.

V. DOPPLER-SHIFTED FREQUENCY MEASUREMENTS

In the previous section the atomic motion was perpendicular to the laser beam propagation when measuring resonant transition frequencies. However, in many experiments the atomic motion is not necessarily perpendicular to the laser beams. In this situation a component of the velocity of the atoms is parallel (or antiparallel) to the laser beam and the frequency of the resonance line becomes Doppler shifted and this Doppler shift depends on the temperature of the atomic oven. Using our method, these Doppler-shifted transition frequencies can be measured and the average velocity of the atoms in the direction of the reference axis and the oven temperature can be determined.

As described earlier when the frequency is detuned from the Doppler-free resonance two pairs of spots move in opposite directions, relating to the pairs of counterpropagating laser beams. To measure the Doppler-shifted wavelengths the earlier setup was adjusted by rotating the oven to form an angle with the lasers. This provided maximum atomic flux for the desired angle, while the cylindrical axis of the atomic oven offered a reference axis to which the spots could be aligned. This scheme is illustrated in Fig. 4. Here the direction of propagation of the laser beams must be taken into account because one pair of the laser beams (2 and 4) makes an acute angle α, while the other pair (beams 1 and 3) forms an obtuse angle β with the reference axis. In both cases the magnitude of the angular difference from $90°$ (and hence the frequency shift) is the same, but the sign is different. To align a pair of spots to the reference axis the laser frequency was detuned from resonance by a certain amount. Blue detuning the laser frequency causes fluorescence spots (corresponding to lasers 2 and 4) to align with the reference axis, while red detuning causes fluorescence spots (from lasers 1 and 3) to align with the

reference axis. Figure 5 demonstrates these Doppler-shifted resonance spots when the angle between the laser and the atomic beam is (a) $\alpha = 70°$ and (c) $\beta = 110°$. A particular advantage of the spot method can be realized in Fig. 5(b), that when on resonance the four spots form a line perpendicular to the laser beams. This allows for the resonant transition frequency to be measured independent of the angle between the laser beam and the atomic beam. The Doppler shift on the resonance frequency depends on the velocity component, of the atoms, parallel (or antiparallel) to the propagation of the lasers, which is dependent upon the cosine of the angle θ between the atomic motion and the propagation of the laser. Therefore the frequency shift, Δf, is given by [34]

$$\Delta f = \frac{f}{c} v \cos \theta, \qquad (1)$$

where f is the Doppler-free transition frequency, c is the speed of light, v is the mean velocity of the atoms along the direction of the reference axis, and θ is the angle between the atom motion and the laser beam. The $v \cos \theta$ term represents the mean velocity component parallel to the laser beam.

The reference axis was rotated to make angles of $63°$, $70°$, $75°$, and $80°$ with one pair of lasers and hence $117°$, $110°$, $105°$, and $100°$ with the other pair of lasers. We measured the Doppler-shifted frequencies when the spots aligned with the reference axis, and our measurements of these frequencies are shown in Fig. 6. Equation (1) was fitted to the data and enables us to derive the average velocity of the atoms in the direction of atomic beam. Using our data we have determined the average atomic velocity to be $260 \pm 20 \text{ ms}^{-1}$ and therefore the temperature of the atomic beam can be estimated.

Using frequencies measured from our technique we were able to photoionize and trap Yb$^+$ isotopes in an ion-trapping experiment [35]. To ionize an Yb atom a 399-nm photon is
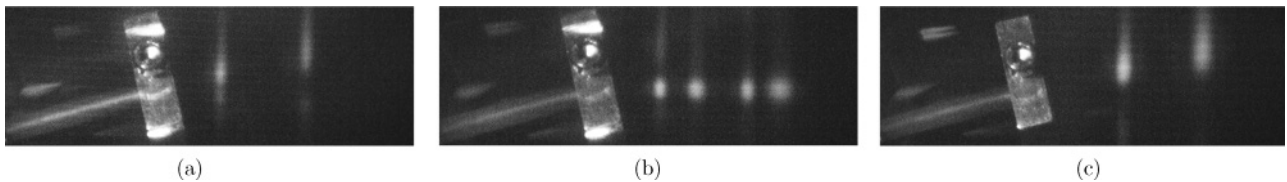

(a)   (b)   (c)

FIG. 5. Pictures show the atomic oven and fluorescence spots where the laser beams intersect the reference axis at (a) $70°$ and (c) $110°$. Panel (b) also demonstrates the non-Doppler-shifted resonance where the spots align perpendicular to the laser beams, as seen in the fluorescence spot technique.
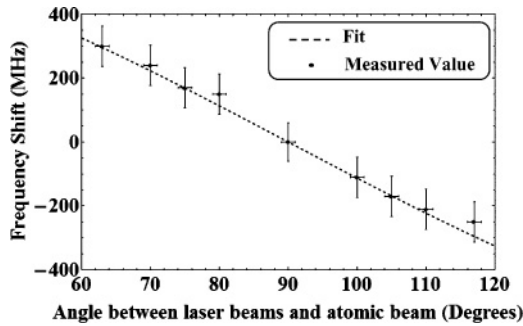
FIG. 6. Doppler frequency shift in the $^1S_0 \leftrightarrow {}^1P_1$ transition of ^{174}Yb as a function of the angle between the laser beams and the atomic beam.

required to drive the $^1S_0 \leftrightarrow {}^1P_1$ transition where a further 369-nm photon excites an electron past the continuum [22,27]. In the ion-trapping experiment the atomic oven and the 399-nm laser made an angle of $63° \pm 2°$. We were able to verify the resonance frequencies for the $^1S_0 \leftrightarrow {}^1P_1$ transitions by photoionization of different Yb isotopes.

VI. CONCLUSION

We have demonstrated a simple technique to determine the resonant transition frequencies and isotope shifts of the 398.91-nm $^1S_0 \leftrightarrow {}^1P_1$ transition for different stable Yb isotopes. We present new values for the resonant frequencies that differ from those of previously published work [29]. Saturation absorption spectroscopy was also performed and the frequencies measured were in good agreement with those obtained via our florescence spot method. The fluorescence spot method has an advantage over absorption saturation spectroscopy as the former method has an easier setup and provides larger signal-to-noise ratios. With small modifications to the setup, the fluorescence spot method can also be used to measure the Doppler-shifted transition frequencies that occur when the laser and the atomic beam are not perpendicular and allowing for predictions of transition frequencies in realistic ion-trap setups. Furthermore, this technique allows us to derive the average thermal velocity of atoms in the direction of the atomic beam.

[1] H. A. Klein, A. Bell, G. Barwood, and P. Gill, Appl. Phys. B **50**, 13 (1990).

[2] H. Lehmitz, J. Hattendorf-Ledwoch, R. Blatt, and H. Harde, Phys. Rev. Lett. **62**, 2108 (1989).

[3] M. Roberts, P. Taylor, G. P. Barwood, P. Gill, H. A. Klein, and W. R. C. Rowley, Phys. Rev. Lett. **78**, 1876 (1997).

[4] V. Enders, P. Courteille, R. Huesmann, L. S. Ma, W. Neuhauser, R. Blatt, and P. E. Toschek, Europhys. Lett. **24**, 325 (1993).

[5] K. Honda, Y. Takahashi, T. Kuwamoto, M. Fujimoto, K. Toyoda, K. Ishikawa, and T. Yabuzaki, Phys. Rev. A **59**, R934 (1999).

[6] U. D. Rapol, A. Krishna, A. Wasan, and V. Natarajan, Eur. Phys. J. D **29**, 409 (2004).

[7] R. Huesmann, C. Balzer, P. Courteille, W. Neuhauser, and P. E. Toschek, Phys. Rev. Lett. **82**, 1611 (1999).

[8] C. S. Edwards, P. Gill, H. A. Klein, A. P. Levick, and W. R. C. Rowley, Appl. Phys. B **59**, 179 (1994).

[9] D. Das and V. Natarajan, Phys. Rev. A **76**, 062505 (2007).

[10] T. Loftus, J. R. Bochinski, and T. W. Mossberg, Phys. Rev. A **63**, 053401 (2001).

[11] R. Maruyama, R. H. Wynar, M. V. Romalis, A. Andalkar, M. D. Swallows, C. E. Pearson, and E. N. Fortson, Phys. Rev. A **68**, 011403 (2003).

[12] C. Tamm, D. Engelke, and V. Bühner, Phys. Rev. A **61**, 053405 (2000).

[13] Z. W. Barber *et al.*, Phys. Rev. Lett. **100**, 103002 (2008).

[14] S. G. Porsev, A. Derevianko, and E. N. Fortson, Phys. Rev. A **69**, 021403 (2004).

[15] T. Hong, C. Cramer, E. Cook, W. Nagourney, and E. N. Fortson, Opt. Lett. **30**, 2644 (2005).

[16] Z. W. Barber, C. W. Hoyt, C. W. Oates, L. Hollberg, A. V. Taichenachev, and V. I. Yudin, Phys. Rev. Lett. **96**, 083002 (2006).

[17] S. J. Park, P. Manson, M. J. Wouters, R. B. Warrington, M. A. Lawn, and P. T. H. Fisk, in *Proceedings of the 2007 IEEE International Frequency Control Symposium—Jointly with The 21st European Frequency and Time Forum*, Vols. 1–4, (IEEE, New York, 2007), pp. 613–616.

[18] M. Roberts, P. Taylor, S. V. Gateva-Kostova, R. B. M. Clarke, W. R. C. Rowley, and P. Gill, Phys. Rev. A **60**, 2867 (1999).

[19] P. J. Blythe, S. A. Webster, H. S. Margolis, S. N. Lea, G. Huang, S.-K. Choi, W. R. C. Rowley, P. Gill, and R. S. Windeler, Phys. Rev. A **67**, 020501 (2003).

[20] C. Tamm, B. Lipphardt, H. Schnatz, R. Wynands, S. Weyers, T. Schneider, and E. Peik, IEEE Trans. Instrum. Meas. **56**, 601 (2007).

[21] S. Olmschenk, K. C. Younge, D. L. Moehring, D. N. Matsukevich, P. Maunz, and C. Monroe, Phys. Rev. A **76**, 052314 (2007).

[22] C. Balzer, A. Braun, T. Hannemann, C. Paape, M. Ettler, W. Neuhauser, and C. Wunderlich, Phys. Rev. A **73**, 041407 (2006).

[23] A. M. Bacon, H. Z. Zhao, L. J. Wang, and J. E. Thomas, Phys. Rev. Lett. **75**, 1296 (1995).

[24] D. DeMille, Phys. Rev. Lett. **74**, 4165 (1995).

[25] R. Hendricks, D. Grant, P. Herskind, A. Dantan, and M. Drewsen, Appl. Phys. B **88**, 507 (2007).

[26] U. Tanaka, H. Matsunishi, I. Morita, and S. Urabe, Appl. Phys. B **81**, 795 (2005).

[27] M. Johanning, A. Braun, D. Eiteneuer, C. Paape, C. Balzer, W. Neuhauser, and C. Wunderlich, e-print arXiv:0712.0969v2 [physics.atom-ph] (2010).

[28] W. F. Meggers and J. L. Tech, J. Res. Natl. Bur. Stand. **83**, 13 (1978).

[29] D. Das, S. Barthwal, A. Banerjee, and V. Natarajan, Phys. Rev. A **72**, 032506 (2005).

[30] T. Loftus, J. R. Bochinski, and T. W. Mossberg, Phys. Rev. A **63**, 023402 (2001).

[31] K. Deilamian, J. D. Gillaspy, and D. E. Kelleher, J. Opt. Soc. Am. B **10**, 789 (1993).

[32] R. Zinkstok, E. J. van Duijn, S. Witte, and W. Hogervorst, J. Phys. B **35**, 2693 (2002).

[33] Yu. Ralchenko, A. E. Kramida, J. Reader, and NIST ASD Team (2008). NIST Atomic Spectra Database (Version 3.1.5), [http://physics.nist.gov/asd3] (2010, August 24).

[34] Harold J. Metcalf and Peter van der Straten, *Laser Cooling and Trapping* (Springer-Verlag, New York Inc., 1999).

[35] J. J. McLoughlin, A. H. Nizamani, J. D. Siverns, R. C. Sterling, M. D. Hughes, B. Stein, B. Lekitsch, S. Weidt, and W. K. Hensinger, e-print arXiv:1007.4010v1 [quant-ph] (2010).